

RESEARCH

Open Access



Single-cell RNA sequencing highlights the role of distinct natural killer subsets in sporadic amyotrophic lateral sclerosis

Esther Álvarez-Sánchez^{1,2}, Álvaro Carbayo^{3,4}, Natalia Valle-Tamayo^{1,2}, Laia Muñoz^{1,2}, Joaquim Aumatell^{1,2}, Soraya Torres^{1,2}, Sara Rubio-Guerra^{1,2}, Jesús García-Castro^{1,2}, Judit Selma-González^{1,2}, Daniel Alcolea^{1,2}, Janina Turon-Sans^{3,4}, Alberto Lleó^{1,2}, Ignacio Illán-Gala^{1,2}, Juan Fortea^{1,2}, Ricard Rojas-García^{3,4} and Oriol Dols-Icardo^{1,2*}

Abstract

Background Neuroinflammation plays a major role in amyotrophic lateral sclerosis (ALS), and cumulative evidence suggests that systemic inflammation and the infiltration of immune cells into the brain contribute to this process. However, no study has investigated the role of peripheral blood immune cells in ALS pathophysiology using single-cell RNA sequencing (scRNAseq).

Methods We aimed to characterize immune cells from blood and identify ALS-related immune alterations at single-cell resolution. For this purpose, peripheral blood mononuclear cells (PBMC) were isolated from 14 ALS patients and 14 cognitively unimpaired healthy individuals (HC), matched by age and gender, and cryopreserved until library preparation and scRNAseq. We analyzed differences in the proportions of PBMC, gene expression, and cell-cell communication patterns between ALS patients and HC, as well as their association with plasma neurofilament light (NfL) concentrations, a surrogate biomarker for neurodegeneration. Flow cytometry was used to validate alterations in cell type proportions.

Results We identified the expansion of CD56^{dim} natural killer (NK) cells in ALS (fold change = 2; adj. *p*-value = 0.0051), mainly driven by a specific subpopulation, NK₂ cells (fold change = 3.12; adj. *p*-value = 0.0001), which represent a mature and cytotoxic CD56^{dim} NK subset. Our results revealed extensive gene expression alterations in NK₂ cells, pointing towards the activation of immune response (adj. *p*-value = 9.2×10^{-11}) and the regulation of lymphocyte proliferation (adj. *p*-value = 6.46×10^{-6}). We also identified gene expression changes in other immune cells, such as classical monocytes, and distinct CD8⁺ effector memory T cells which suggested enhanced antigen presentation via major histocompatibility class-II (adj. *p*-value = 1.23×10^{-8}) in ALS. The inference of cell-cell communication patterns demonstrated that the interaction between HLA-E and CD94:NKG2C from different lymphocytes to NK₂ cells is unique to ALS blood compared to HC. Finally, regression analysis revealed that the proportion of CD56^{bright} NK cells along with the ALSFRS-r, disease duration, and gender, explained up to 76.4% of the variance in plasma NfL levels.

*Correspondence:
Oriol Dols-Icardo
odols@santpau.cat

Full list of author information is available at the end of the article



© The Author(s) 2025. **Open Access** This article is licensed under a Creative Commons Attribution-NonCommercial-NoDerivatives 4.0 International License, which permits any non-commercial use, sharing, distribution and reproduction in any medium or format, as long as you give appropriate credit to the original author(s) and the source, provide a link to the Creative Commons licence, and indicate if you modified the licensed material. You do not have permission under this licence to share adapted material derived from this article or parts of it. The images or other third party material in this article are included in the article's Creative Commons licence, unless indicated otherwise in a credit line to the material. If material is not included in the article's Creative Commons licence and your intended use is not permitted by statutory regulation or exceeds the permitted use, you will need to obtain permission directly from the copyright holder. To view a copy of this licence, visit <http://creativecommons.org/licenses/by-nc-nd/4.0/>.

Conclusion Our results reveal a signature of relevant changes occurring in peripheral blood immune cells in ALS and underscore alterations in the proportion, gene expression, and signaling patterns of a cytotoxic and terminally differentiated CD56^{dim} NK subpopulation (NK₂), as well as a possible role of CD56^{bright} NK cells in neurodegeneration.

Keywords ALS, scRNAseq, Immune system, Natural killer cells, Neurodegeneration

Background

Amyotrophic lateral sclerosis (ALS) is a neurodegenerative disease characterized by the loss of upper and lower motor neurons leading to progressive muscle weakness, wasting, and paralysis that result in death within three to five years from disease onset [1]. Neuroinflammation plays a major role in the pathophysiology of ALS [2]. Cumulative evidence suggests that systemic inflammation and peripheral blood immune cells contribute to neuroinflammation and are a major hallmark of neurodegenerative diseases, including ALS [3]. Previous studies have demonstrated alterations in the proportions of immune cells in the blood of ALS patients using flow cytometry [4–6], including Natural Killer (NK) cells [4, 7]. However, flow cytometry relies on a list of preselected antibodies, limiting the ability to identify cell subpopulations without bias. As a consequence, over the years, researchers have agreed on the stratification of NK cells into two major subpopulations with different characteristics and functions in immunity. These NK subpopulations have been dichotomized based on the expression of CD56, resulting in NK cells with high CD56 expression (CD56^{bright}) and those with intermediate to low CD56 levels (CD56^{dim}) [8]. In contrast, single-cell RNA sequencing (scRNAseq) represents an unbiased high-throughput technology that does not rely on a predefined panel of markers and offers unprecedented resolution for feasibly determining the entire landscape of cell populations and subpopulations. Furthermore, scRNAseq has the potential to uncover differential gene expression changes and cell-cell communication alterations that emerge in response to disease conditions at single-cell resolution. However, a thorough investigation of peripheral blood mononuclear cells (PBMC) using scRNAseq in ALS is still lacking. In this study, we characterized PBMC isolated from 14 ALS patients not carrying disease-causing mutations and 14 cognitively unimpaired healthy control (HC) individuals using scRNAseq. Our aim was to characterize the peripheral immune cell compartment, identify alterations in PBMC proportions, uncover a signature of gene expression changes, and investigate cell-cell communication patterns associated with ALS pathophysiology.

Methods

Study participants

The diagnosis was made by experienced neurologists fulfilling El Escorial revised criteria for definite ALS [9]. All

patients underwent a cognitive and behavioral screening that included a separate interview with a reliable informant and the administration of the Edinburgh Cognitive and Behavioral ALS Screen (ECAS). None of the ALS patients showed signs of cognitive or behavioral impairment at the time of inclusion in this study and mutations in known ALS/Frontotemporal dementia-causing genes were ruled out using a custom panel. Clinical variables included age at disease onset, age at blood extraction, disease duration at the time of sampling, region of onset of motor symptoms (categorized as spinal or bulbar), and the ALS Functional Rating Scale-Revised (ALSFRRS-r) at the time of blood sampling. All ALS patients were treated with Riluzole since their diagnosis as part of standard care management, receiving a stable dose of 100 mg per day. Plasma samples were obtained for 13 out of the 14 ALS patients to determine the concentrations of Neurofilament light (NfL) using the Simoa SR-X platform (Quanterix). All HC participants were evaluated by experienced neurologists [10]. Briefly, they had scores between 27 and 30 on the Mini-Mental State Examination (MMSE) test, absence of subjective memory complaints or objective memory deficits with a scalar score equal to or greater than eight (measured with the Free and Cued Selective Reminding Test - FCSRT) and a score on the Clinical Dementia Rating scale (CDR) of 0. In addition, levels of core Alzheimer's disease biomarkers in cerebrospinal fluid (obtained the same day of the PBMC isolation) were within the normal range in all HC [10]. All participants with concomitant autoimmune and/or infectious diseases, vaccinated within the last month of blood extraction, or being treated with anti-inflammatory drugs were excluded. Demographic data for HC participants included gender, date of birth, and age at blood extraction.

PBMC isolation

All blood samples were collected in EDTA tubes, stored at 4 °C, and processed 60 min after blood extraction. PBMCs were isolated through Ficoll gradient density centrifugation. A total of 10 mL were mixed with 10 mL of RPMI1640, layered onto SepMate-50 (IVD) tubes (Stem-Cell) prefilled with 15 mL of Ficoll-Paque Plus (Cytiva), and centrifuged at 800 g for 15 min without acceleration and brake. After two washes with RPMI1640, PBMCs were diluted to a density of 1×10^6 cells/mL in freezing media consisting of RPMI1640 with 10% DMSO, 20% FBS, and penicillin-streptomycin 1:1000 (Lonza),

gradually frozen using a freezing box (Mr. Frosty) for at least 24 h at -80°C and transferred to liquid nitrogen for cryopreservation.

Single-cell RNA sequencing

Cryopreserved PBMCs were thawed in a water bath at 37°C and transferred to a 15 mL Falcon tube containing 10 mL of pre-warmed RPMI media supplemented with 10% FBS (Thermo Fisher Scientific). Samples were centrifuged at 350 g for 5 min at room temperature (RT), supernatant was removed, and pellets were resuspended with 1 mL of cold 1X PBS (Thermo Fisher Scientific) supplemented with 0.05% BSA (MACS Miltenyi Biotec) and 0.1 mg/mL of DNase I (PN LS002007, Worthington-Biochem), and incubated 10 min at RT. Cells were filtered with a 40 μm strainer (Cell Strainer), washed with 10 mL of PBS + 0.05% BSA, centrifuged, and finally resuspended in 1 mL of PBS + 0.05% BSA. Cell concentration and viability were verified with a TC20™ Automated Cell Counter (Bio-Rad Laboratories, S.A) upon staining of the cells with Trypan Blue.

Cells from eight different PBMCs samples were pooled following the Cell Multiplexing Oligo Labeling for Single Cell RNA Sequencing Protocol (10x Genomics). A total of four PBMCs pools were processed. Briefly, between one and two million cells from each sample were resuspended in 100 μL of Cell Multiplexing Oligo (3' CellPlex Kit, 10x Genomics) and incubated at RT for 5 min. Cells were washed 3 times with cold 1X PBS supplemented with 1% BSA, all centrifugations being performed at 350 g at 4°C for 5 min. Cells were finally resuspended in an appropriate volume of 1X PBS-0.05% BSA in order to obtain a final cell concentration of approximately 1000 cells/ μL and counted using a TC20™ Automated Cell Counter. Samples were mixed with a 50:50 ratio, and the resulting pools were filtered with a 40 μm strainer and checked for final cell number and viability before loading onto the Chromium. The Cellplex pools were partitioned into 3' Gel Bead Emulsions with a Target Cell Recovery of 20,000 cells (corresponding to 2,500 cells per sample within each plex), loaded in two replicates to obtain a total of 5,000 cells per sample.

Libraries were prepared following 10x Genomics Single Cell 3' mRNA kit protocol with Feature Barcode technology for Cell Multiplexing. Briefly, after GEM-RT clean-up, cDNA from poly-adenylated mRNA and barcoded DNA from the CMO Feature Barcode were amplified via PCR according to the Target Recovery cell number. A SPRI selection clean-up was done to separate the amplified cDNA molecules for 3' Gene Expression (GEX) and the CMO-derived cDNA (CellPlex). 100 ng of mRNA-derived cDNA were used for GEX library construction while 5 μL of CMO-derived cDNA were used to amplify the corresponding Cellplex library. Size distribution

and library concentration were determined using a Bioanalyzer High Sensitivity chip (Agilent Technologies). Sequencing was carried out on a NovaSeq6000 system (Illumina) to obtain approximately 40,000 reads per cell for the GEX library and 2,000–4,000 reads per cell for the Cellplex library.

Data processing

We processed all raw sequencing reads with Cell Ranger v7.0.1 and mapped them to the GRCh38 human genome. At the sample level, ambient RNA was removed using DecontX [11]. Subsequent quality control steps were performed using Seurat v4 [12] and v5 [13]. Low-quality cells were removed if they contained a percentage of mitochondrial reads above the 98th percentile in our samples (that is $>20.706\%$), or above the 98th or below the 2nd percentile of unique genes detected (that is 3235.178 and 340.633, respectively). Samples were grouped into each of the eight sequencing plexes (that is four main plexes with two replicates each), and doublets removed using DoubletFinder [14].

Finally, all samples were merged into a single object, and data normalized using the function `NormalizeData`. Using Seurat v5, we used the function `RunAzimuth` to annotate cells based on a PBMC reference dataset (“pbmcref”), which represents a multimodal reference atlas of PBMC with established cell subtype markers [13]. We used layer 2 and layer 3 of the reference PBMC dataset, containing 25 and 55 immune cell subpopulations, respectively. Finally, we split data into layers based on each subplex and integrated data through the `IntegrateLayers` function.

Differential gene expression and cell-type proportions

The Seurat function `FindMarkers` was used to identify differentially expressed genes by comparing the gene expression profiles of all cells within each cluster between the ALS and HC groups. To test for significance, MAST was selected as it uses a hurdle model to effectively address the sparsity and bimodal expression distributions typical of scRNAseq data. Genes expressed in at least 10% of cells were tested. Gender, age at sample collection, plex, and percentage of mitochondrial and ribosomal reads were included as latent variables. There was no difference in these variables across groups. As recommended in Seurat, p -values were corrected using Bonferroni based on the total number of genes in the dataset. Genes with an adjusted p -value less than 0.05 and average log-fold change greater than 0.25 were considered as differentially expressed. To perform gene ontology (GO) and Kyoto Encyclopedia of Genes and Genomes (KEGG) pathway enrichment analyses, we used Metascape 3.5 (metascape.org), applying default parameters (minimum overlap=3, p value cutoff=0.01, and minimum

enrichment = 1.5). Differences in cell-type proportions were assessed using “propeller”, within the “speckle” package [15] and considered significant if $FDR < 0.05$, as reported by propeller.

Inference of cell-cell communication

Cell-cell interaction patterns were assessed using CellChat (v2.1.0) [16] based on the expression of known ligand-receptor pairs. CellChat infers the communication probability of ligand-receptor pairs between two different cell types and determines significance based on whether the communication probability between these two cell types is statistically greater than in randomly permuted cell groups.

Flow cytometry

PBMCs were processed in seven separate runs, each including the same number of ALS patients and HC (PBMCs from two ALS and two HC participants). PBMCs were thawed at 37 °C and resuspended in 10 mL of RPMI1640 supplemented with 10% FBS. Cells were centrifuged at 300 g for 5 min and washed once with 10 mL of RPMI1640 + 10% FBS and once with 10 mL of flow cytometry buffer (1X PBS + 0.5% BSA + 2 mM EDTA). PBMCs were resuspended in 80 µL of flow cytometry buffer and Fc receptors were blocked with 20 µL of FcR Blocking Reagent (Miltenyi Biotec) for 10 min at 4 °C. Cells were stained with antibody cocktails and Viability 405/520 Fixable Dye (Miltenyi Biotec) in 100 µL of flow cytometry buffer in the dark for 15 min. Fluorophore-conjugated antibodies were used as follows: CD56 Antibody (PE-Vio[®] 770, REAfinity, Miltenyi Biotec), CD3 Antibody (Vio[®] Bright R720, REAfinity, Miltenyi Biotec), and CD16 Antibody (Brilliant Violet 570™, BioLegend). After incubation, PBMCs were washed with 1 mL of flow cytometry buffer and centrifuged at 300 g for 5 min. Cells were then fixed and permeabilized using the Inside Stain Kit (Miltenyi Biotec) following the manufacturer’s instructions. Then, cells were stained with Milli-Mark[®] Anti-FcεRI Antibody, γ subunit-FITC (Merck) and incubated in the dark for 10 min. PBMCs were centrifuged at 300 g for 5 min and resuspended in 250 µL of flow cytometry buffer. Samples were analyzed with the MACSQuant[®] Analyzer 16 Flow Cytometer, and cell type proportions and fluorescence intensities were determined using the MACSQuantify software (Miltenyi Biotec). Fluorescence Minus One (FMO) controls were used to define the appropriate gating threshold for each marker. FMO controls were prepared for each fluorochrome by staining cells with all antibodies except the one of interest, using PBMCs from two ALS patients and two HC (Supplementary Fig. 1 and Supplementary Fig. 2). Doublets and debris were first excluded. NK cells were identified within the lymphocyte population (based on FSC

and SSC values) as CD3⁻ and CD56⁺. Then, based on the expression of the CD56 marker, NK cells were divided into CD56^{dim} NK cells and CD56^{bright} NK cells. Finally, according to the expression levels of the intracellular protein FcεR1G in CD56^{dim} NK cells, we identified CD56^{dim} FcεR1G⁺ NK cells (corresponding to the NK_2 subset) (see Supplementary Fig. 3 and Supplementary Fig. 4). As we gated PBMCs, neutrophils and other granulocytes were excluded from our samples. Therefore, monocytes were selected from the total PBMC population based on FSC and SSC values, and classical monocytes were identified based on the absence of CD16 expression (CD16⁻ monocytes or classical monocytes) (Supplementary Fig. 5 and Supplementary Fig. 6).

A model for predicting plasma NFL levels

To determine whether the neurodegeneration signature of ALS patients, determined using plasma neurofilament light (NFL) levels as a surrogate biomarker, could be explained by other relevant variables, we considered a set of candidate predictor variables, which included demographic factors (age at sample collection and gender), clinical measures (disease duration and ALSFRS-r at the time of blood sampling, and age at onset), and the proportions of NK_2, CD56^{bright} NK cells and classical monocytes (obtained from our scRNAseq data). We aimed to identify the optimal model using the stepAIC function within the package “MASS”. The stepAIC function performs a bidirectional stepwise model selection by iteratively adding or removing predictors based on changes in the AIC (Akaike Information Criterion) to minimize the AIC value in order to find the most parsimonious one and at the same time identifying the best model approximating the levels of NFL. The bidirectional stepwise regression combines the advantages of backward and forward methods, and allows the model to be evaluated and revisited, while addressing overfitting or redundancy (a limitation of backward or forward regression). We further computed indices of model quality and goodness of fit using the package “performance”. The optimal model was validated using the proportion of CD56^{bright} NK cells obtained using flow cytometry. All analyses were performed in R.

Statistical analysis

The Shapiro-Wilk test (shapiro.test function) was used to assess data normality and Mann-Whitney U (wilcox.test function) to test for differences between groups (“stats” R package). For correlation analyses, we determined the Spearman correlation coefficient using the ggscatter function within the “ggpubr” R package. Differences were considered significant at $p \leq 0.05$ and all statistical tests were two-sided. All analyses were performed in R.

Results

Expansion of peripheral immune cells in the blood of ALS patients

A total of 108,833 PBMCs from 14 ALS patients and 14 cognitively unimpaired healthy controls (HC) passed quality control (QC). There were no differences in age at sample acquisition (57.6 years (SD = 5.3) in ALS and 59 years (SD = 8.3) in HC) or gender (10 females were included in each group, 71.4%) between patients and HC. The group of ALS patients had an average age at disease onset of 56.4 years and an average disease duration at the time of sampling of 14 months (Table 1). Detailed demographic and clinical information is included in Supplementary Table 1.

We first aimed to identify alterations in major PBMC populations associated with ALS. Therefore, PBMC were initially classified into one of the 25 annotated major cell populations defined in the second layer of the multimodal PBMC reference included in Azimuth (Fig. 1A). CD56^{dim} Natural Killer (CD56^{dim} NK) cells were increased in the blood of ALS patients (fold change = 2; adj. *p*-value = 0.0051) (Fig. 1B). We also found that CD14 monocytes (also known as classical monocytes) were expanded in the ALS blood, however, our analyses did not reach statistical significance after correction for multiple comparisons (fold change = 1.48; *p*-value = 0.025; adj. *p*-value = 0.36). Notably, we also identified a trend towards an increased proportion of CD56^{bright} Natural Killer (CD56^{bright} NK) cells in ALS patients (fold change = 1.79; *p*-value = 0.072; adj. *p*-value = 0.44) (Fig. 1B). We did not find alterations in the other cell types identified in this study after correcting for multiple comparisons (Supplementary Table 2 provides the proportions of all cell types across all samples).

We then aimed to gain a deeper resolution by clustering our PBMC dataset into the 55 immune cell populations included in the most comprehensive layer of the pbmcres multimodal dataset (layer 3) (Fig. 2A). Our results demonstrated that the expansion of a specific CD56^{dim} NK subpopulation, referred to as NK_2 (fold change = 3.12; adj. *p*-value = 1×10^{-4}), drives the elevation of CD56^{dim} NK cells in ALS (Fig. 2B). In addition, we observed the upregulation of a less frequent subpopulation

of CD56^{dim} NK cells (NK_4, fold change = 2.21; adj. *p*-value = 2.3×10^{-3}), representing less than 1% of total PBMCs (Fig. 2B). As expected, the proportions of CD14 monocytes and NK CD56^{bright} cells did not change in this more detailed approach, revealing differences similar than those mentioned above. We did not find alterations in the other cell subtypes identified in this study after correcting for multiple comparisons (Supplementary Table 3 provides the proportions of all cell subpopulations across all samples). We did not find any statistically significant correlation between the proportion of the 55 immune cell subtypes and disease duration, plasma NfL levels or the ALSFRS-r after correcting for multiple comparisons. The most upregulated cell subtype, NK_2, is characterized by the higher expression of cytotoxic molecules (such as *GZMB*), NK cell maturity markers (such as *FCER1G*, *NKG7*, or *SPON2*), as well as *FCRG3A* (CD16), indicating that it is the most mature and terminally differentiated CD56^{dim} NK subset (Fig. 2C). On the other hand, CD56^{bright} NK cells expressed the highest levels of *NCAM1* (CD56), *XCL1*, *XCL2* and *GZMK*; followed by NK_4 cells, characterized by the intermediate expression of these markers (*NCAM1* (CD56), *XCL1*, *XCL2* and *GZMK*), thus suggesting that NK_4 belong to a transitional state from CD56^{bright} to CD56^{dim} NK cells (Fig. 2C).

Extensive gene expression alterations in NK_2 and other immune cell populations in ALS

We focused our analyses on the deepest Azimuth cell-type resolution layer (layer 3, containing 55 immune cell types). Our analyses of differential gene expression at cellular resolution revealed that NK cells were the most altered cell type. Among them, NK_1 and NK_2 showed the highest number of deregulated genes (adj. *p*-value < 0.05, 40 and 37, respectively), underscoring the key role of NK_2 cells in ALS. The most significant gene expression alterations in NK_2 cells from ALS patients included the upregulation of *FCER1G* (adj. *p*-value = 7.32×10^{-67} , fold change = 1.31) and *TYROBP* (adj. *p*-value = 1.39×10^{-64} , fold change = 1.3) (Fig. 3A). Gene ontology and pathway enrichment analyses pointed towards the regulation of cell activation (GO:0050865; adj. *p*-value = 1.41×10^{-7}) in NK_1, while implying the activation of immune response (GO:0002253; adj. *p*-value = 9.2×10^{-11}) and the regulation of lymphocyte proliferation (GO:0050670; adj. *p*-value = 6.46×10^{-6}) in NK_2 cells. We also identified 42 genes significantly deregulated in CD14 monocytes, highlighting the downregulation of inflammasome activation-related genes, such as *TMEM176B* (adj. *p*-value = 1.07×10^{-135} , fold change = -0.79) and *TMEM176A* (adj. *p*-value = 9.51×10^{-87} , fold change = 0.71) (Fig. 3B). Strikingly, four distinct subpopulations of CD8 effector

Table 1 Clinical and demographic characteristics of ALS patients and HC

	ALS (n = 14)	HC (n = 14)
Gender, n Female (%)	10 (71.4)	10 (71.4)
Age at Sampling, mean (years) (SD)	57.6 (5.3)	59 (8.3)
Onset Region, n Spinal (%)	8 (57.1)	-
Age at onset, mean (years) (SD)	56.4 (5.3)	-
Disease duration (months) (SD)	14 (6.1)	-

Age at onset and at sample acquisition is shown in years while disease duration in months

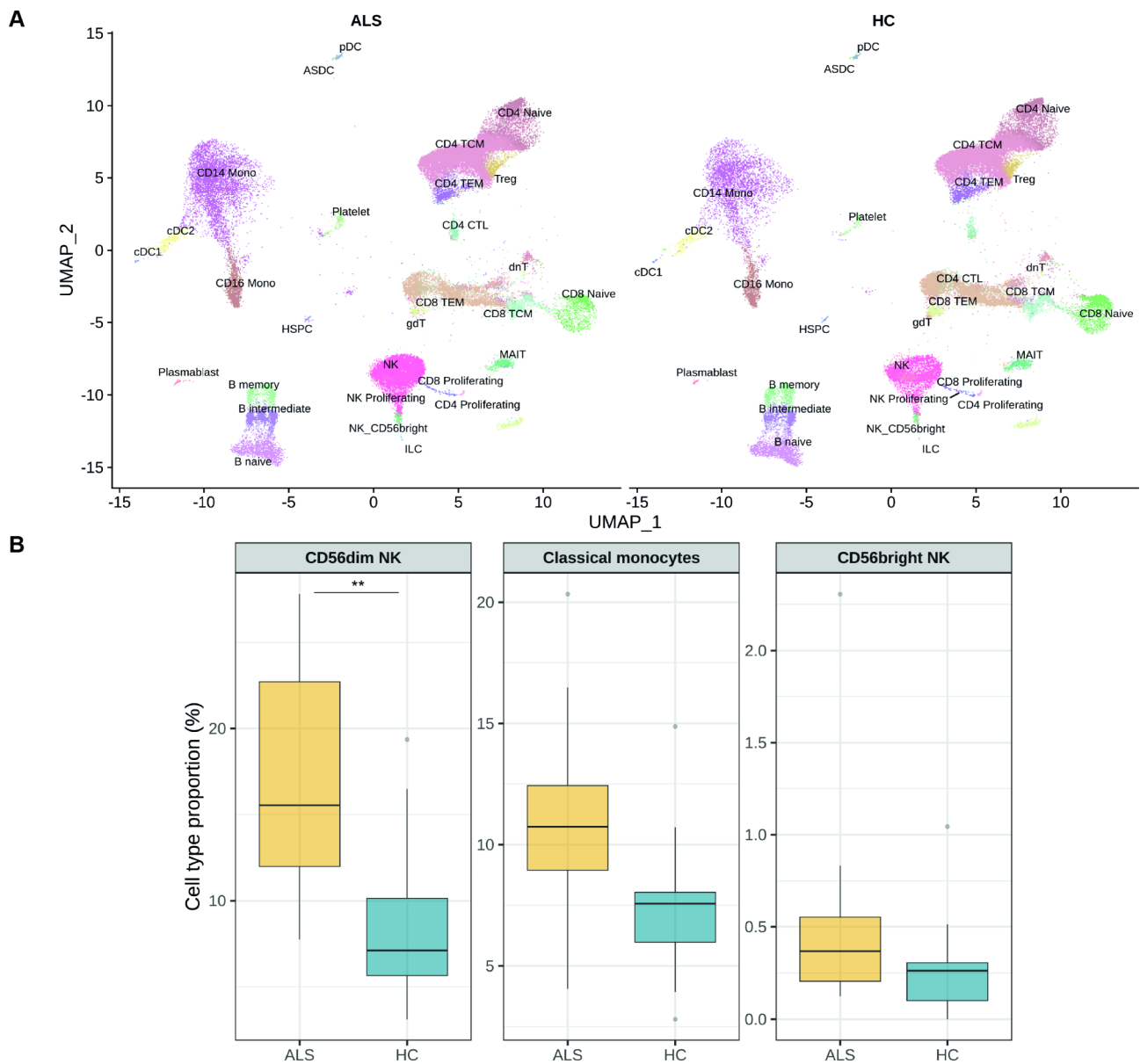


Fig. 1 Alterations in the proportions of major peripheral blood mononuclear cell populations in ALS. **(A)** UMAP plot indicating the clusters of major PBMC populations in ALS and HC. Note that in this plot, CD56^{dim} NK cells are named as NK. **(B)** Box plot showing the significant expansion of CD56^{dim} NK cells, and the upregulation of classical monocytes and CD56^{bright} NK cells. Cell type proportions were calculated by propeller tool based on the total number of cells per sample that passed quality control after scRNAseq. PBMC: peripheral blood mononuclear cells; NK: CD56^{dim} NK cell; DC: dendritic cell; Mono: Monocyte; TCM: central memory T cell. TEM: effector memory T cell; gdT: gamma-delta T cell; HSPC: Hematopoietic stem and progenitor cell; MAIT: Mucosal-associated invariant T cell; dnT: double-negative T cell. ** adjusted *p*-value < 0.01

memory T cells showed extensive upregulation of genes involved in antigen processing and presentation (such as *HLA-DPB1*, *HLA-DPA1*, *CD74* or *HLA-DRB1*), in particular CD8⁺ effector memory T cells 5 (CD8 TEM₅) (Fig. 3C), suggesting enhanced antigen presentation via major histocompatibility class-II (GO:0019886; adj. *p*-value = 1.23 × 10⁻⁸). (See Supplementary Table 4 for a list of significant differential gene expression changes across all cell subtypes).

Inference of cell-cell communication patterns

We first aimed to compare the interaction strength of outgoing and incoming signaling between ALS and HC in different cell subtypes. Our analysis demonstrated changes in NK₂ cells, with more than a 3-fold increase in signal reception in ALS compared to HC (Fig. 4A). The increased interaction strength in signal reception in NK₂ cells was driven by major histocompatibility complex I (MHC-I) pathways, although the C-type lectin (CLEC) and CD99 pathways also exhibited minor

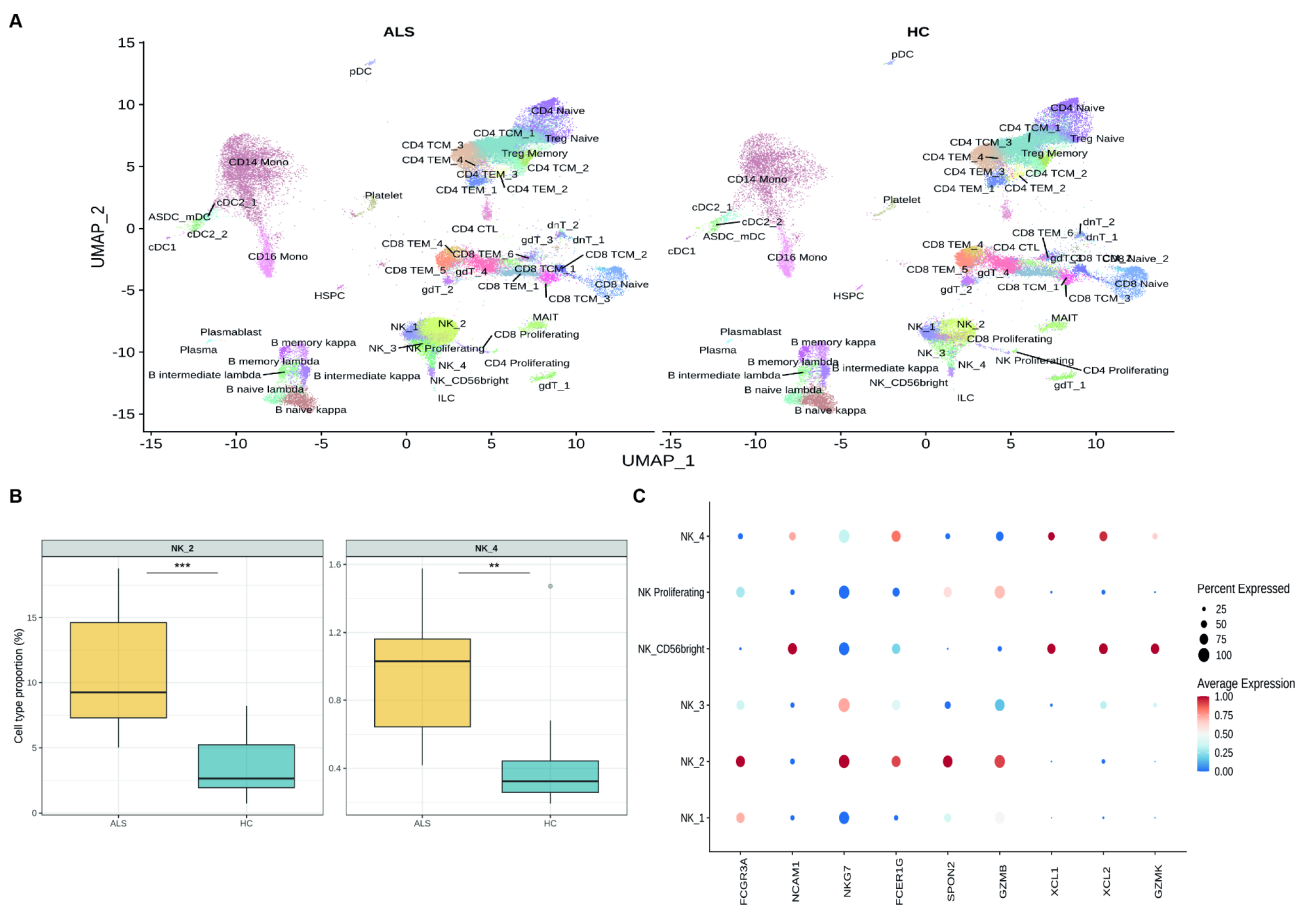


Fig. 2 Two NK subtypes drive the expansion of CD56dim NK cells in ALS. **(A)** UMAP plot showing the clusters of PBMC subpopulations in ALS and HC. **(B)** Box plot demonstrating that NK_2 cells and NK_4 cells are expanded in the blood of ALS patients. **(C)** Dot plot depicting the expression of the traditional FCGR3A (CD16) and NCAM1 (CD56), together with 7 other marker genes across subsets of human blood NK cells. Cell type proportions were calculated by propeller tool based on the total number of cells per sample that passed quality control after scRNAseq. PBMC: peripheral blood mononuclear cells; NK: CD56dim NK cell; DC: dendritic cell; Mono: Monocyte; TCM: central memory T cell. TEM: effector memory T cell; gdT: gamma-delta T cell; HSPC: Hematopoietic stem and progenitor cell; MAIT: Mucosal-associated invariant T cell; dnT: double-negative T cell. **adjusted p -value < 0.01, *** adjusted p -value < 0.001

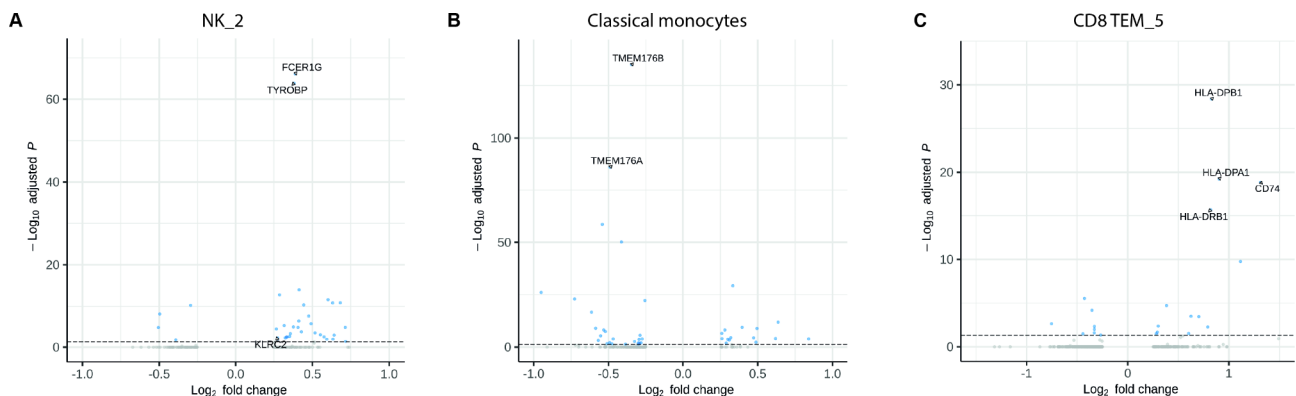


Fig. 3 Most relevant gene expression alterations in peripheral blood mononuclear cells from ALS patients. Volcano plots displaying differentially expressed genes between the ALS and HC. The vertical axis (y-axis) corresponds to the $-\log_{10}$ adjusted p value, and the horizontal axis (x-axis) represents the \log_2 fold change value obtained. Significantly differentially expressed genes are depicted with blue circles (adjusted p -value < 0.05), whereas gray circles display the nonsignificant genes. **(A)** Volcano plot displaying differentially expressed genes between the ALS and HC groups in NK_2 cells. **(B)** Volcano plot showing differentially expressed genes between the ALS and HC groups in classical monocytes. **(C)** Volcano plot displaying differentially expressed genes between the ALS and HC groups in CD8 TEM_5 cells. The most significant and interesting genes are depicted. PBMC: peripheral blood mononuclear cells. NK_2: CD56^{dim} NK cell subtype 2; TEM: effector memory T cell.

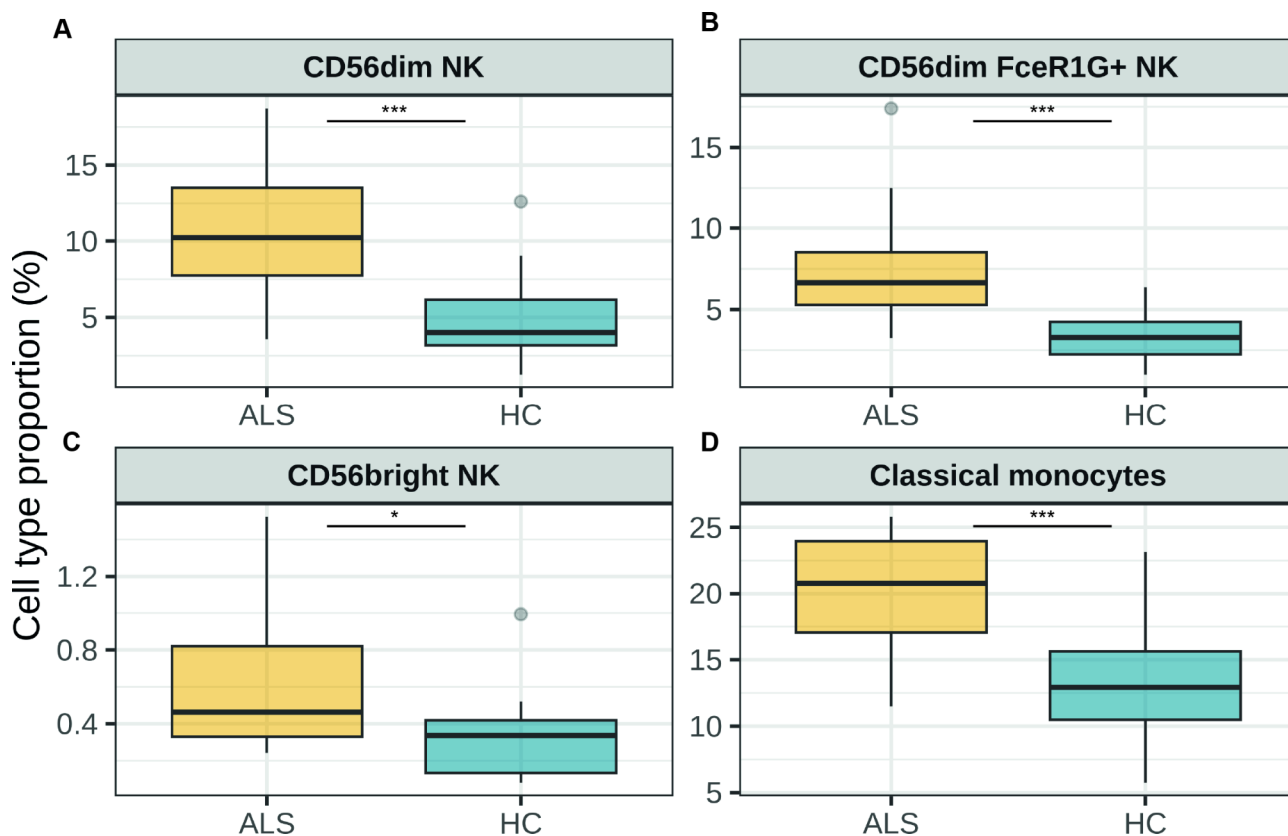


Fig. 5 Validation of alterations in cell type proportions using flow cytometry. Box plot demonstrating that (A) CD56^{dim} NK cells, (B) CD56^{dim} FceR1G+ NK cells, (C) CD56^{bright} NK cells and (D) classical monocytes are expanded in ALS blood. Cell type proportions are calculated based on the total number of gated peripheral blood mononuclear cells per sample. * *p*-value < 0.05, *** *p*-value < 0.001

Regression modeling implicates CD56^{bright} NK cells in neurodegeneration

The concentration of plasma NfL was higher in ALS patients compared to HC (46.87 pg/mL vs. 7.40 pg/mL; $p = 4.08 \times 10^{-5}$) (Supplementary Table 1) and directly correlated with disease duration ($\rho = 0.57$; $p = 0.043$). However, we did not find a statistically significant correlation between plasma NfL levels, the ALSFRS-r or the proportion of the 55 immune cell subpopulations identified in this study. Given the key role of the cytotoxic and mature CD56^{dim} NK subset identified in this study (NK_2), the expansion of CD56^{bright} NK cells and classical monocytes in the blood of ALS patients, together with their increased capability to infiltrate into the central nervous system (CNS) [17–19], we sought to explore whether these cell subtypes could explain the neurodegeneration signature of ALS patients using plasma NfL concentrations as a surrogate biomarker. We also considered a set of candidate predictor variables, which included demographic factors (age at sample collection and gender), clinical measures (disease duration and ALSFRS-r at the time of blood sampling, and age at onset). The optimal regression model, which was both the most parsimonious and the best at approximating NfL levels, included

disease duration, gender, ALSFRS-r, and the proportion of CD56^{bright} NK cells, while ruling out the contribution of other variables:

$$\text{NfL} \sim \text{disease duration} + \text{gender} + \text{ALSFRS-r} + \text{CD56}^{\text{bright}} \text{ NK cells}$$

The optimal regression model explained 64.5% of the variance in plasma NfL levels ($R^2 = 0.7635$; adjusted $R^2 = 0.6452$; $p = 0.012$). Next, we aimed to validate this result using the proportion of CD56^{bright} NK cells obtained using flow cytometry. Our analysis demonstrated that the obtained regression model was able to explain 76.4% of plasma NfL levels ($R^2 = 0.842$; adjusted $R^2 = 0.7637$; $p = 0.0027$), highlighting the relationship between CD56^{bright} NK cells and neurodegeneration in ALS (Supplementary Table 6 contains indices of model performance for both the discovery and validation regression models).

Discussion

This is the first study to assess the role of PBMCs in ALS using an unbiased high-throughput technology at the resolution of single cells (scRNAseq). Our study highlights the key role of NK cells in the pathophysiology of ALS and describes relevant alterations in gene expression, as

well as unique cell-cell communication patterns associated with this neurodegenerative disease.

Previous studies have implicated CD56^{dim} NK cells using flow cytometry in ALS [4, 7]. However, their methodology precluded the precise identification of the diversity of CD56^{dim} NK cell subtypes and limited the accurate delineation of their unique molecular hallmarks (gene expression and cell-cell communication) in an unbiased manner. In recent years, single-cell technologies have revolutionized the field and boosted the characterization of cellular subpopulations. Initially, we confirmed the association of NK cells with ALS, particularly with CD56^{dim} NK cells [4, 7]. Leveraging the unbiased, and high-resolution nature of our scRNAseq dataset, we further refined this observation. For the first time, our results demonstrate that a unique CD56^{dim} NK cell subset (referred to as NK_2) is strongly expanded in ALS and drives the previously described increase of CD56^{dim} NK cells in this neurodegenerative disease [4, 7]. We confirmed this result by flow cytometry using the FcεR1G antibody to confidently determine the presence and proportion of NK_2 cells (CD56^{dim} FcεR1G + NK cells). The NK_2 subpopulation is a mature, cytotoxic, and terminally differentiated NK cell subtype characterized by the high expression of *NKG7*, *FCER1G*, or *SPON2*. Importantly, two recent and relevant studies have focused their attention on delineating the molecular characteristics of NK subgroups in hundreds of individuals and distinct tissues using a combination of scRNAseq and CITE-seq (20, 21). Our NK_2 subtype is concordant with these reports, which name this NK subset as NK1C [20] or late CD56^{dim} NK cells [21]. Furthermore, for the first time, using both scRNAseq and flow cytometry, our results reveal the upregulation of CD56^{bright} NK cells and support the previously reported increase of classical monocytes (CD14 monocytes) in ALS [4, 19]. Collectively, our data provide evidence of ALS-related immune dysregulation in peripheral blood, highlighting NK_2 cells as the main drivers of CD56^{dim} NK cell expansion in ALS.

Beyond their upregulation, classical monocytes represented the most altered cell subtype at the gene expression level. The top two deregulated genes in classical monocytes were strongly downregulated (*TMEM106A* and *TMEM106B*) in ALS. Interestingly, *TMEM176B* is a negative regulator of inflammasome activation, and inhibition of its encoded protein (TMEM176B) enhances NLRP3 blockage, improving antitumor immunity [22]. On the other hand, downregulation of both *TMEM106A* and *TMEM106B* has been recently demonstrated in *MAPT* mutation carriers, although in that case, the difference was reported in non-classical monocytes, which were reduced in the blood of people with familial tauopathy [23]. Therefore, decreased expression of these genes is common in ALS and familial tauopathy; however, the

difference between these two neurodegenerative conditions is only observed at the cell-type level (classical monocytes in ALS and non-classical monocytes in familial tauopathy). These data highlight the relevance of studying gene expression at the resolution of single cells, as such differences might be hidden when studying bulk tissues. Among other gene expression alterations, we underscore the enhanced ability of distinct subpopulations of CD8+ effector memory T cells, especially CD8 TEM_5, to present antigens, as demonstrated by the marked upregulation of major histocompatibility complex II (MHC-II) genes (such as *HLA-DPB1*, *HLA-DPA1*, *HLA-DRB1* and *CD74*) in these cells from ALS patients. The CD74 receptor, known as the MHC-II invariant chain, acts as a class II molecular chaperone in its canonical function [24]. Together with MHC class II molecules, CD74 is primarily expressed on specialized antigen-presenting cells such as dendritic cells, B cells, and macrophages. However, these molecules can also be expressed by some subsets of activated and terminally differentiated T cells. In fact, recent data suggest that CD74 is abundantly expressed intracellularly in T cells and is upregulated following T-cell activation [25]. Furthermore, as an alternative function, the extracellular domain of CD74 is known to bind the macrophage migration inhibitory factor (MIF), promoting activation and regulating the chemotaxis of T cells [24–26]. Therefore, our results suggest that the expression of CD74 is enhanced in CD8+ effector memory T cells from ALS patients and, beyond reflecting their higher activation profile, the increased expression might promote the infiltration of CD8+ T cells to other tissues.

In addition, the expression of MHC class II markers in T cells is known to be a consequence of prolonged activation and induce clonal anergy, leading to functional inactivation and non-proliferative states of these cells [27]. As a consequence, the overexpression of MHC class II markers in CD8+ effector memory T cells from ALS patients might indicate that these cells are unresponsive or have transitioned into an anergic or even senescent state. However, functional studies are needed to confirm these hypotheses. Altogether, our results provide a signature of gene expression alterations at single-cell resolution that might suggest novel therapeutic targets based on cell-based interceptive medicine or chimeric antigen receptor (CAR)-T/NK cell therapies to tune the peripheral immune system in ALS.

We also aimed to determine whether plasma NfL levels could be predicted by the proportions of significantly increased cell subtypes identified in our study (NK_2, CD56^{bright} NK cells, and classical monocytes), along with other clinical and demographic variables. Our regression model disclosed that CD56^{bright} NK cells (together with disease duration, gender, and ALSFRS-r, known to impact

on ALS and its progression [28]) explain more than 75% of the variance in plasma NfL concentrations. Therefore, our data suggest that CD56^{bright} NK cells play a role in ALS-related neurodegeneration and should be investigated in future research studies. Importantly, CD56^{bright} NK cells express Nkp46 at high levels, and Nkp46+ NK cells have recently been detected in the motor cortex and spinal cord of ALS patients [29]. These cells have been shown to infiltrate the CNS, contribute to neurodegeneration, and modulate the microglial phenotype in ALS [29], potentially linking these functions to the association reported in our study. Thus, our results indicate that the proportion of CD56^{bright} NK cells determined in a non-invasive biofluid might reflect neurodegenerative changes. In addition, previous studies have demonstrated the presence of NK cells in the human brain with discordant outcomes. In Lewy-Body related diseases, a study demonstrated that NK cells have a protective role by clearing alpha-synuclein deposits and that their systemic depletion enhances alpha-synuclein deposition in a mouse model [30]. On the other hand, the accumulation of NK cells in the aging brain impairs neurogenesis and exacerbates cognitive decline [31]. However, the precise role of NK cells and, particularly, of their subpopulations remains to be elucidated in ALS. Overall, our results and previous data suggest that the proportion of CD56^{bright} NK cells in the blood might parallel neurodegenerative changes in the motor cortex and/or spinal cord, enhancing the prediction of neurodegeneration from an accessible biofluid.

The inference of cell-cell communication patterns revealed the increased reception of signals by NK₂ cells, driven by the MHC-I pathway and specifically through the interaction of HLA-E (T lymphocytes) with CD94:NKG2C (NK₂ cells). Strikingly, our results demonstrate that this signaling pattern is unique to ALS blood compared to HC. The CD94/NKG2C heterodimeric activating receptor binds to non-classical MHC class IB molecules, such as HLA-E, and this interaction activates and triggers NK cell cytotoxicity against other cell types [32]. Importantly, peptide-HLA-E complexes bind CD94/NKG2C (activating) but also CD94/NKG2A (inhibitory) in a peptide dependent manner, showing higher affinity for the inhibitory receptor [33]. Conversely, a recent study has characterized the repertoire of HLA-E presented CD94/NKG2X ligands. Their results demonstrate that certain peptides selectively activate NK cells through CD94/NKG2C and, importantly, these peptide-HLA-E complexes do not bind the inhibitory receptor despite its traditionally suggested higher affinity [34]. Therefore, modulating the heterodimeric CD94/NKG2C activating receptor and characterizing the landscape of HLA-E-presented peptides could suggest and represent novel therapeutic strategies for ALS. Furthermore, it

is widely known that NK cells participate in innate and adaptive immunity, and also modulate T cells responses [35]. Accordingly, changes in gene expression found in NK₂ cells pointed towards the increased activation of immunity and regulation of lymphocyte proliferation in ALS patients, as demonstrated by the top enriched GO terms from the list of upregulated genes. Notably, the NK₂ subset is characterized by the high expression of *FCER1G*, recently shown to be key in promoting T-cell exhaustion and limiting CD8+ T cell responses by NK cells [36]. Our results highlight that NK₂ cells may be key players in controlling the peripheral immune response in ALS.

Altogether, the expansion, gene expression and cell-cell communication alterations of NK₂ cells in ALS blood, and the association of CD56^{bright} NK cells with neurodegeneration may have important implications for the design of therapeutic strategies aimed at depleting or modifying NK cells. Until now, all studies have focused on blocking the whole population of NK cells or targeting the major population of CD56^{dim} NK cells, leading to conflicting findings in ALS and other neurodegenerative diseases [29–31, 37, 38]. Our results suggest that: (1) a specific and cytotoxic CD56^{dim} NK cell subset (NK₂) play a key role in regulating the peripheral immune response and (2) CD56^{bright} NK cells may infiltrate the CNS or, at least, directly contribute to neurodegenerative processes in ALS. Therefore, NK cell-based therapeutics should consider the diverse and specialized subpopulations of cells to appropriately and successfully achieve the desired impact on the modulation of the peripheral immune compartment.

Our study has some limitations. First, it is important to note that neutrophils have been previously associated with ALS [39, 40]. However, the isolation of PBMCs have precluded the inclusion of neutrophils and other granulocytes in this study, preventing us from confirming this finding using our scRNAseq dataset. In addition, although our study represents the largest investigation of the peripheral immune system in ALS using scRNAseq, the low number of ALS patients and HC included herein has limited our ability to assess the impact of age or sex on the immune cell profile in ALS. In this context, the determination of inflammatory biomarkers and their impact on the peripheral immune cell profile could provide valuable insights into the role of systemic inflammation in ALS and its association with clinical variables. However, larger cohorts with multimodal biomarker data are needed to test these hypotheses. Although we used an unbiased high-throughput technology and included a well-characterized group of ALS patients and HC, as well as a large number of PBMCs per participant, it is important to confirm our findings in other cohorts. In fact, our study suggests that the peripheral immune system

and NK cells play a role in ALS. However, further validation is needed by including disease controls, such as patients with other motor neuron diseases (e.g. spinal muscular atrophy) or neurodegenerative diseases (e.g. frontotemporal dementia) to confirm disease specificity. In addition, the impact of ongoing ALS treatment on the peripheral immune profile should be evaluated using non-human models, as including untreated ALS patients as controls would not comply with the standards of care. Moreover, our findings are primarily associative; therefore, future functional studies are needed to confirm the impact of the peripheral immune system on ALS. Investigating the role of immune cells in the CSF could establish a direct relationship between the peripheral immune system and other cell subtypes in ALS, as recently described [41]. Notably, none of the ALS patients carried mutations in any known disease-causing gene. While this group of patients represents more than 90% of all ALS cases, it will be relevant to assess whether the alterations reported in our study are generalizable to genetic forms of ALS. Finally, evaluating alterations in the peripheral immune system longitudinally would provide valuable insights into the role of immune cells during disease progression.

Conclusions

Our study strongly supports the role of NK cells in ALS and, for the first time, highlights that a cytotoxic and terminally differentiated CD56^{dim} NK subtype (NK₂ or CD56^{dim} FcεR1G + NK) drives NK cell expansion and exhibits relevant gene expression and cell-cell communication alterations associated with ALS. In addition, our data suggest that CD56^{bright} NK cells, which have an enhanced potential to infiltrate into tissues, influence neurodegeneration. We also underscore alterations in the proportion of other immune cells (classical monocytes) and describe a signature of gene expression changes beyond NK₂ cells (such as in classical monocytes and diverse subpopulations CD8 + effector memory T cells). Our study provides compelling evidence that peripheral immune cells play a major role in ALS pathophysiology and highlights the importance of studying well-defined cell subpopulations to disentangle their precise roles in health and disease, as well as to effectively design novel therapies aimed at modulating the peripheral immune system for the treatment of neurodegenerative diseases.

Abbreviations

ALS	Amyotrophic lateral sclerosis
ALSFRS-r	ALS Functional Rating Scale-Revised
HC	Cognitively unimpaired healthy controls
nfl	Neurofilament light
NK	Natural killer
PBMC	Peripheral blood mononuclear cells
scRNAseq	Single-cell RNA sequencing

Supplementary Information

The online version contains supplementary material available at <https://doi.org/10.1186/s12974-025-03347-0>.

Supplementary Material 1

Supplementary Material 2

Acknowledgements

We thank the Single Cell Genomics group (Centro Nacional de Análisis Genómico) for library preparation and single-cell RNA sequencing procedures. We are grateful to the staff of the flow cytometry platform (Marta Soler and Lia Ros) of Institut de Recerca Sant Pau for expert advice related to flow cytometry. We thank the patients and their families for their contributions to this study.

Author contributions

O.D.-I., J.F. and R.R.-G. conceptualized and designed the study. E.A.-S., A.C. N-V-T., L.M., J.A., S.T., J.T.-S., D.A., A.L., J.G.-C., J.S.-G., S.R.-G., I.I.-G., J.F., R.R.-G. and O.D.-I. participated in data acquisition. E.A.-S., J.A. and O.D.-I. analyzed all data. E.A.-S., D.A., A.L., J.F., R.R.-G. and O.D.-I. wrote the manuscript. All authors contributed to and approved the final version of the manuscript.

Funding

This study was funded by the Instituto de Salud Carlos III (Ministerio de Asuntos Económicos y Transformación Digital, Gobierno de España) through the projects P18/00326, P121/01395 (and associated F122/00077 to N.V.-T. and O.D.-I.) and P124/01087 to O.D.-I.; P119/01543, P123/00845 to R.R.-G., P121/00791, P124/00598 to I.I.-G., and INT21/00073, P120/01473 and P123/01786 to J.F., and the Centro de Investigación Biomédica en Red sobre Enfermedades Neurodegenerativas Program 1, cofounded by the European Regional Development Fund/European Social Fund (ERDF/ESF), 'A way to make Europe'/'Investing in your future'. O.D.-I. receives funding from the Fundación Española para el Fomento de la Investigación de la Esclerosis Lateral Amiotrófica (FUNDELA - 'Por un mundo sin ELA'), Fundación HNA ('Premio Investigación científica de salud'), the Alzheimer's Association (AARF-22-924456) and the Fondation Jérôme Lejeune (PDC-2023-51; #202307). I.I.-G. is a senior Atlantic Fellow for Equity in Brain Health at the Global Brain Health Institute (GBHI), and receives funding from the GBHI, the Alzheimer's Association, and the Alzheimer Society (GBHI ALZ UK-21-720973 and AACSF-21-850193). I.I.-G. was also supported by the Juan Rodés Contract (JR20/0018). This work was also supported by the National Institutes of Health grants (R01 AG056850; R21 AG056974, R01 AG061566, R01 AG081394 and R61 AG066543 to J.F.), the Department de Salut de la Generalitat de Catalunya, Pla Estratègic de Recerca i Innovació en Salut (SLT006/17/00119 to J.F.).

Data availability

The datasets used and analyzed during the current study are available from the corresponding author on reasonable request.

Declarations

Ethics approval and consent to participate

The study was approved by the ethics committee of Hospital Sant Pau and adhered to the standards for medical research involving humans as recommended by the Declaration of Helsinki. All participants and/or their legal representatives signed the written informed consent.

Consent for publication

Not applicable.

Competing interests

The authors declare no competing interests.

Author details

¹Memory Unit, Neurology Department and Institut de Recerca Sant Pau, Hospital de la Santa Creu i Sant Pau, Universitat Autònoma de Barcelona, Sant Quintí 77-79, 08041 Barcelona, Spain

²Network Center for Biomedical Research in Neurodegenerative Diseases (CIBERNED), Madrid, Spain

³Network Center for Biomedical Research in Rare Diseases (CIBERER), Madrid, Spain

⁴Neuromuscular Diseases Unit, Department of Neurology, Hospital de la Santa Creu i Sant Pau, Institut de Recerca Sant Pau, Universitat Autònoma de Barcelona, Sant Quintí 77-79, 08041 Barcelona, Spain

Received: 13 November 2024 / Accepted: 15 January 2025

Published online: 23 January 2025

References

- Kiernan MC, Vucic S, Talbot K, McDermott CJ, Hardiman O, Shefner JM, Al-Chalabi A, Huynh W, Cudkovic M, Talman P, et al. Improving clinical trial outcomes in amyotrophic lateral sclerosis. *Nat Rev Neurol*. 2021;17(2):104–18.
- Dols-Icardo O, Montal V, Sirisi S, López-Pernas G, Cervera-Carles L, Querol-Vilaseca M, Muñoz L, Belbin O, Alcolea D, Molina-Porcel L, et al. Motor cortex transcriptome reveals microglial key events in amyotrophic lateral sclerosis. *Neurol Neuroimmunol Neuroinflamm*. 2020;7(5):e829.
- Berriat F, Lobsiger CS, Boillée S. The contribution of the peripheral immune system to neurodegeneration. *Nat Neurosci*. 2023;26(6):942–54.
- Murdock BJ, Zhou T, Kashlan SR, Little RJ, Goutman SA, Feldman EL. Correlation of peripheral immunity with rapid amyotrophic lateral sclerosis progression. *JAMA Neurol*. 2017;74(12):1446–54.
- Beers DR, Henkel JS, Zhao W, Wang J, Huang A, Wen S, Liao B, Appel SH. Endogenous regulatory T lymphocytes ameliorate amyotrophic lateral sclerosis in mice and correlate with disease progression in patients with amyotrophic lateral sclerosis. *Brain*. 2011;134(Pt 5):1293–314.
- Murdock BJ, Bender DE, Kashlan SR, Figueroa-Romero C, Backus C, Callaghan BC, Goutman SA, Feldman EL. Increased ratio of circulating neutrophils to monocytes in amyotrophic lateral sclerosis. *Neurol Neuroimmunol Neuroinflamm*. 2016;3(4):e242.
- Murdock BJ, Famie JP, Piecuch CE, Pawlowski KD, Mendelson FE, Pieroni CH, Iniguez SD, Zhao L, Goutman SA, Feldman EL. NK cells associate with ALS in a sex- and age-dependent manner. *JCI Insight*. 2021;6(11):e147129.
- Freud AG, Mundy-Bosse BL, Yu J, Caligiuri MA. The broad spectrum of human natural killer cell diversity. *Immunity*. 2017;47(5):820–33.
- Brooks BR, Miller RG, Swash M, Munsat TL. El Escorial revisited: revised criteria for the diagnosis of amyotrophic lateral sclerosis. *Amyotroph Lateral Scler Other Mot Neuron Disord*. 2000;1(5):293–9.
- Alcolea D, Clarimón J, Carmona-Iragui M, Illán-Gala I, Morenas-Rodríguez E, Barroeta I, Ribosa-Nogué R, Sala I, Sánchez-Saudinós MB, Videla L, et al. The Sant Pau Initiative on Neurodegeneration (SPIN) cohort: a data set for biomarker discovery and validation in neurodegenerative disorders. *Alzheimers Dement (N Y)*. 2019;5:597–609.
- Yang S, Corbett SE, Koga Y, Wang Z, Johnson WE, Yajima M, Campbell JD. Decontamination of ambient RNA in single-cell RNA-seq with DecontX. *Genome Biol*. 2020;21(1):57.
- Hao Y, Hao S, Andersen-Nissen E, Mauck WM 3rd, Zheng S, Butler A, Lee MJ, Wilk AJ, Darby C, Zager M, et al. Integrated analysis of multimodal single-cell data. *Cell*. 2021;184(13):3573–e358729.
- Hao Y, Stuart T, Kowalski MH, Choudhary S, Hoffman P, Hartman A, Srivastava A, Molla G, Madad S, Fernandez-Granda C, et al. Dictionary learning for integrative, multimodal and scalable single-cell analysis. *Nat Biotechnol*. 2024;42(2):293–304.
- McGinnis CS, Murrow LM, Gartner ZJ, DoubletFinder. Doublet detection in single-cell RNA sequencing data using artificial nearest neighbors. *Cell Syst*. 2019;8(4):329–e3374.
- Phipson B, Sim CB, Porrello ER, Hewitt AW, Powell J, Oshlack A. Propeller: testing for differences in cell type proportions in single cell data. *Bioinformatics*. 2022;38(18):4720–6.
- Jin S, Guerrero-Juarez CF, Zhang L, Chang I, Ramos R, Kuan CH, Myung P, Plikus MV, Nie Q. Inference and analysis of cell-cell communication using CellChat. *Nat Commun*. 2021;12(1):1088.
- Rodríguez-Mogeda C, van Ansenwoude CMJ, van der Molen L, Stribis EMM, Mebius RE, de Vries HE. The role of CD56bright NK cells in neurodegenerative disorders. *J Neuroinflammation*. 2024;21(1):48.
- Ning Z, Liu Y, Guo D, Lin WJ, Tang Y. Natural killer cells in the central nervous system. *Cell Commun Signal*. 2023;21(1):341.
- Zondler L, Müller K, Khalaji S, Bliedehäuser C, Ruf WP, Grozdanov V, Thiemann M, Fundel-Clemes K, Freischmidt A, Holzmann K, et al. Peripheral monocytes are functionally altered and invade the CNS in ALS patients. *Acta Neuropathol*. 2016;132(3):391–411.
- Rebuffet L, Melsen JE, Escalière B, Basurto-Lozada D, Bhandoola A, Björkström NK, Bryceson YT, Castriconi R, Cichocki F, Colonna M, et al. High-dimensional single-cell analysis of human natural killer cell heterogeneity. *Nat Immunol*. 2024;25(8):1474–88.
- Netskar H, Pfefferle A, Goodridge JP, Sohlberg E, Dufva O, Teichmann SA, Brownlie D, Michaëlsson J, Marquardt N, Clancy T, et al. Pan-cancer profiling of tumor-infiltrating natural killer cells through transcriptional reference mapping. *Nat Immunol*. 2024;25(8):1445–59.
- Segovia M, Russo S, Jeldres M, Mahmoud YD, Perez V, Duhalde M, Charnet P, Rousset M, Victoria S, Veigas F, et al. Targeting TMEM176B enhances antitumor immunity and augments the efficacy of immune checkpoint blockers by unleashing inflammasome activation. *Cancer Cell*. 2019;35(5):767–e7816.
- Sirkis DW, Warly Solsberg C, Johnson TP, Bonham LW, Sturm VE, Lee SE, Rankin KP, Rosen HJ, Boxer AL, Seeley WW, et al. Single-cell RNA-seq reveals alterations in peripheral CX3CR1 and nonclassical monocytes in familial tauopathy. *Genome Med*. 2023;15(1):53.
- Schröder B. The multifaceted roles of the invariant chain CD74—more than just a chaperone. *Biochim Biophys Acta*. 2016;1863(6 Pt A):1269–81.
- Zhang L, Woltering I, Holzner M, Brandhofer M, Schaefer CC, Bushati G, Ebert S, Yang B, Muenchhoff M, Hellmuth JC, et al. CD74 is a functional MIF receptor on activated CD4+ T cells. *Cell Mol Life Sci*. 2024;81(1):296.
- Leng L, Metz CN, Fang Y, Xu J, Donnelly S, Baugh J, Delohery T, Chen Y, Mitchell RA, Bucala R. MIF signal transduction initiated by binding to CD74. *J Exp Med*. 2003;197(11):1467–76.
- Pichler WJ, Wyss-Coray T. T cells as antigen-presenting cells. *Immunol Today*. 1994;15(7):312–5.
- Goutman SA, Hardiman O, Al-Chalabi A, Chiò A, Savelieff MG, Kiernan MC, Feldman EL. Recent advances in the diagnosis and prognosis of amyotrophic lateral sclerosis. *Lancet Neurol*. 2022;21(5):480–93.
- Garofalo S, Coccoza G, Porzia A, Inghilleri M, Raspa M, Scavizzi F, Aronica E, Bernardini G, Peng L, Ransohoff RM, et al. Natural killer cells modulate motor neuron-immune cell cross talk in models of amyotrophic lateral sclerosis. *Nat Commun*. 2020;11(1):1773.
- Earls RH, Menees KB, Chung J, Gutekunst CA, Lee HJ, Hazim MG, Rada B, Wood LB, Lee JK. NK cells clear α -synuclein and the depletion of NK cells exacerbates synuclein pathology in a mouse model of α -synucleinopathy. *Proc Natl Acad Sci U S A*. 2020;117(3):1762–71.
- Jin WN, Shi K, He W, Sun JH, Van Kaer L, Shi FD, Liu Q. Neuroblast senescence in the aged brain augments natural killer cell cytotoxicity leading to impaired neurogenesis and cognition. *Nat Neurosci*. 2021;24(1):61–73.
- Braud VM, Allan DS, O'Callaghan CA, Söderström K, D'Andrea A, Ogg GS, Lazetic S, Young NT, Bell JI, Phillips JH, et al. HLA-E binds to natural killer cell receptors CD94/NKG2A, B and C. *Nature*. 1998;391(6669):795–9.
- Valés-Gómez M, Reyburn HT, Erskine RA, López-Botet M, Strominger JL. Kinetics and peptide dependency of the binding of the inhibitory NK receptor CD94/NKG2-A and the activating receptor CD94/NKG2-C to HLA-E. *EMBO J*. 1999;18(15):4250–60.
- Huisman BD, Guan N, Rückert T, Garner L, Singh NK, McMichael AJ, Gillespie GM, Romagnani C, Birnbaum ME. High-throughput characterization of HLA-E-presented CD94/NKG2x ligands reveals peptides which modulate NK cell activation. *Nat Commun*. 2023;14(1):4809.
- Crouse J, Xu HC, Lang PA, Oxenius A. NK cells regulating T cell responses: mechanisms and outcome. *Trends Immunol*. 2015;36(1):49–58.
- Duhan V, Hamdan TA, Xu HC, Shinde P, Bhat H, Li F, Al-Matary Y, Häussinger D, Bezgovsek J, Friedrich SK, et al. NK cell-intrinsic Fc ϵ R γ limits CD8+ T-cell expansion and thereby turns an acute into a chronic viral infection. *PLoS Pathog*. 2019;15(6):e1007797.
- Komine O, Yamashita H, Fujimori-Tonou N, Koike M, Jin S, Moriwaki Y, Endo F, Watanabe S, Uematsu S, Akira S, et al. Innate immune adaptor TRIF deficiency accelerates disease progression of ALS mice with accumulation of aberrantly activated astrocytes. *Cell Death Differ*. 2018;25(12):2130–46.
- Zhang Y, Fung ITH, Sankar P, Chen X, Robison LS, Ye L, D'Souza SS, Salinero AE, Kuentzel ML, Chittur SV, et al. Depletion of NK cells improves cognitive function in the Alzheimer Disease mouse model. *J Immunol*. 2020;205(2):502–10.
- McGill RB, Steyn FJ, Ngo ST, Thorpe KA, Heggie S, Ruitenber MJ, Henderson RD, McCombe PA, Woodruff TM. Monocytes and neutrophils are associated with clinical features in amyotrophic lateral sclerosis. *Brain Commun*. 2020;2(1):fcaa013.

40. Cao W, Cao Z, Tian Y, Zhang L, Wang W, Tang L, Xu C, Fan D. Neutrophils are associated with higher risk of incident amyotrophic lateral sclerosis in a BMI- and age-dependent manner. *Ann Neurol*. 2023;94(5):942–54.
41. Kim HJ, Ban JJ, Kang J, Im HR, Ko SH, Sung JJ, Park SH, Park JE, Choi SJ. Single-cell analysis reveals expanded CD8+GZMKhigh T cells in CSF and shared peripheral clones in sporadic amyotrophic lateral sclerosis. *Brain Commun*. 2024;6(6):fcae428.

Publisher's note

Springer Nature remains neutral with regard to jurisdictional claims in published maps and institutional affiliations.